Available online at www.sciencedirect.com
SCIENCE DIRECT®
Acta Materialia 52 (2004) 667–674
Acta MATERIALIA
www.actamat-journals.com

Thermodynamics, enthalpy relaxation and fragility of the bulk metallic glass-forming liquid $Pd_{43}Ni_{10}Cu_{27}P_{20}$

G.J. Fan [a,*], J.F. Löffler [a,b], R.K. Wunderlich [c], H.-J. Fecht [c,d]

[a] *Department of Chemical Engineering and Materials Science, University of California, Davis, CA 95616, USA*
[b] *Laboratory of Metal Physics and Technology, Department of Materials, ETH Zürich, CH-8092 Zürich, Switzerland*
[c] *Materials Division, University of Ulm, 89081 Ulm, Germany*
[d] *Research Center Karlsruhe, Institute of Nanotechnology, 76021 Karlsruhe, Germany*

Received 29 January 2003; received in revised form 9 July 2003; accepted 1 October 2003

Abstract

Thermodynamic properties, enthalpy relaxation and fragility of a $Pd_{43}Ni_{10}Cu_{27}P_{20}$ bulk metallic glass-forming liquid have been investigated and the thermodynamic functions been calculated. The enthalpy relaxation from the amorphous state into the equilibrium supercooled liquid state was found to follow a stretched exponential function with the relaxation time obeying an Arrhenius law. The fragility index, calculated from the heating rate dependence of T_g, yields a value of 65. The excellent glass-forming ability of this alloy is attributed to a smaller thermodynamic driving force and larger diffusion length for crystallization than in other bulk metallic glass-forming alloys.

Keywords: Bulk metallic glasses; Thermodynamics; Relaxation; Fragility

1. Introduction

When a liquid is cooled from the melting point at a certain cooling rate, it either crystallizes or undercools. If crystal nucleation does not happen due to kinetic constraints, the equilibrium supercooled liquid can eventually be cooled to a temperature, at which the liquid fails to reach the equilibrium at experimental time scales and becomes a glass [1]. A good glass former is expected to have a small thermodynamic driving force and sluggish kinetics for crystal nucleation [2,3]. The thermodynamic properties of a glass start to deviate from their equilibrium values at the glass transition temperature. However, the thermodynamic properties, among which the enthalpy can be directly measured, relax towards their equilibrium values if the glass is isothermally annealed in the vicinity of T_g [4].

Metallic liquids are generally not stable over an extended temperature range in the supercooled liquid, making it difficult and in most cases impossible to determine their thermodynamic properties, for example specific heat capacity. During the past decade, a new family of bulk metallic glass-forming liquids was discovered, including La–Al–Ni [5], Mg–Cu–Y [6], Zr–Ni–Al–Cu [7], Zr–Ti–Cu–Ni–Be [8], Pd–Ni–Cu–P [9], (Fe, Co)–Si–Al–Ga–P [10], Nd–Fe–Co–Al [11], etc. which exhibit good thermal stability and a wide supercooled liquid range before crystallization. These findings provide the possibility to experimentally measure the thermodynamic properties in bulk metallic glasses [2,12,13]. So far, the $Pd_{43}Ni_{10}Cu_{27}P_{20}$ alloy shows the best glass-forming ability with a critical cooling rate as low as 0.01 K/s [14].

In this paper, the specific heat capacities of the $Pd_{43}Ni_{10}Cu_{27}P_{20}$ alloy both in the supercooled liquid region as well as in the amorphous and crystalline state have been measured and the thermodynamic properties been calculated. The long-time annealing of this glass in the vicinity of the glass transition temperature did not result in crystallization and phase separation. Thus, the enthalpy relaxation behavior could be studied successfully and the relaxation time was found to follow an

* Corresponding author. Tel.: +1-530-754-8998; fax: +1-530-752-9554.
E-mail address: gfan@ucdavis.edu (G.J. Fan).

1359-6454/$30.00 © 2003 Acta Materialia Inc. Published by Elsevier Ltd. All rights reserved.
doi:10.1016/j.actamat.2003.10.003

Arrhenius law below T_g with an apparent activation energy of 3.96 eV. The good glass-forming ability of the $Pd_{43}Ni_{10}Cu_{27}P_{20}$ alloy is attributed to a small Gibbs free energy difference between the supercooled liquid and the crystalline state as well as to a large diffusion length necessary for crystallization.

2. Experimental

The $Pd_{43}Ni_{10}Cu_{27}P_{20}$ alloy was prepared by induction melting of the pure elemental metals and phosphorus under ultrahigh purity argon atmosphere in a quartz glass tube. The samples were subsequently fluxed in B_2O_3 at 1300 K for 0.5 h followed by water quenching. The amorphicity of the samples was verified by X-ray diffraction measurements. The composition of the samples was confirmed by wavelength-dispersive X-ray analysis. To ensure the same configurational state of the amorphous samples, the as-cast samples were heated up to 610 K at a heating rate $R_h = 0.167$ K/s and subsequently cooled to room temperature with a cooling rate $R_c = 0.167$ K/s.

A differential scanning calorimeter (Perkin–Elmer DSC 7) was used to study the thermodynamic properties and the enthalpy relaxation of the glassy samples. The samples were protected against oxidation by a constant flow of high-purity argon. By comparing with the specific heat capacity of a sapphire standard sample, the specific heat capacity of the amorphous state, supercooled liquid state, and the crystalline state was measured using DSC (see for example [15]).

The enthalpy relaxation of the amorphous samples was investigated by isothermal annealing of specimens at $T = 569$, 565, 561, and 557 K, respectively, for different times, t. During the isothermal annealing, the amorphous samples relax towards lower enthalpic states with increasing t and eventually towards the equilibrium state after a very long time of annealing. After annealing, the specimens were cooled with $R_c = 0.167$ K/s to ambient temperature and then heated with $R_h = 0.167$ K/s through the glass transition to recover the enthalpy lost during the previous isothermal annealing experiment.

To determine the true heating rate dependence of the calorimetric glass transition temperature, $T_g^{on}(R_h)$, the instrument specific response function was evaluated from the heating rate dependence of the onset temperatures of melting of indium and zinc standards. For low heating rates, a large sample mass of approximately 100 mg was used to obtain a distinct signal.

3. Results

Fig. 1 shows a DSC scan of a $Pd_{43}Ni_{10}Cu_{27}P_{20}$ specimen with $R_h = 0.167$ K/s. The glass transition is observed at $T_g = 576$ K. The onset temperature for crystallization is at $T_x = 660$ K and the supercooled liquid range extends to $T_x - T_g = 84$ K. The exothermic reaction due to melting of the alloy starts at $T_m = 790$ K and the enthalpy of fusion was evaluated as $\Delta H_f = 7.2$ kJ/mol. This compares well with $\Delta H_f = 7.01$ kJ/mol, obtained by Lu et al. [14].

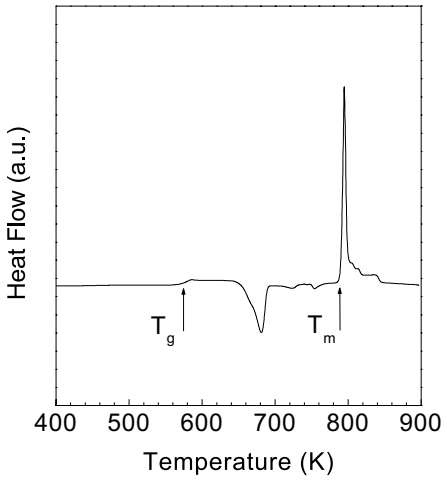

Fig. 1. DSC scan of a $Pd_{43}Ni_{10}Cu_{27}P_{20}$ bulk metallic glass sample performed with $R_h = 0.167$ K/s.

The specific heat capacities of the amorphous phase, $C_p^{am.}$, supercooled liquid, C_p^{l}, and crystalline phase, C_p^{x}, are shown in Fig. 2 as a function of temperature. These results agree well with those of other Pd-based bulk metallic glasses [13,14]. Furthermore, a jump in the specific heat capacity is observed in Fig. 2 when the amorphous phase relaxes into the supercooled liquid state. As proposed by Angell [16], such a jump in specific heat capacity is associated with the fragility of the glass-forming liquid. A fragile liquid has less stable structures

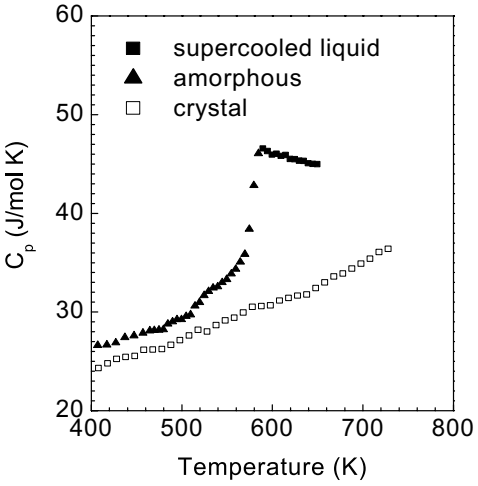

Fig. 2. Specific heat capacity of $Pd_{43}Ni_{10}Cu_{27}P_{20}$ in the supercooled liquid, amorphous, and crystalline state as a function of temperature.

than a strong liquid when it solidifies to a glass. Thus, a fragile liquid has a larger configurational specific heat capacity than a strong liquid, leading to a larger difference in the specific heat capacity between the supercooled liquid and the glass. Accordingly, the larger the specific heat capacity jump is around the glass transition, the more fragile is the liquid.

The enthalpy of a glass at a certain temperature T may deviate from its equilibrium value $H_T^{\text{eq.}}$, since some additional enthalpy can be trapped when the glass forms. Long-time annealing of the glass at that temperature (10 or 20 K below the calorimetric glass transition) will result in the loss of this additional enthalpy and the glass gradually relaxes into the equilibrium supercooled liquid state. The enthalpy of the glass that was lost during the isothermal annealing can be recovered by a subsequent DSC scan of the annealed sample, resulting in an overshoot in the DSC signal in reference to the unrelaxed sample. The enthalpy recovery $\Delta H_T(t)$ during the DSC scan is equal to the enthalpy relaxed during the isothermal annealing experiment. Fig. 3 shows a series of DSC scans with $R_h = 0.167$ K/s for glasses annealed at $T = 569$ K with different annealing times. An overshoot in the DSC heat flow signal, depending on t, can be clearly observed. The corresponding enthalpy recovery $\Delta H_T(t)$ is shown in Fig. 4; $\Delta H_T(t)$ increases gradually as a function of t and saturates for $t > 3000$ s. The time dependence of $\Delta H_T(t)$ cannot be fitted by a simple exponential relaxation function, which shows that the enthalpy relaxation of the $Pd_{43}Ni_{10}Cu_{27}P_{20}$ liquid does not involve a single Debye relaxation event. However, it can well be fitted by a stretched exponential relaxation function

$$\Delta H_T(t) = \Delta H_T^{\text{eq.}}\left\{1 - \exp\left[-\left(\frac{t}{\tau}\right)^{\beta}\right]\right\}, \quad (1)$$

where $\Delta H_T^{\text{eq.}}$ is the equilibrium value of $\Delta H_T(t)$ for $t \to \infty$ at the annealing temperature T, τ is the relaxation time and $\beta < 1$ is the Kohlrausch exponent [17]. The latter indicates a broad distribution of Debye relaxation times originating from the inhomogeneity of the supercooled liquid [18]. The fitting of the experimental data with Eq. (1) yields $T = 569$ K, $\Delta H_T^{\text{eq.}} = 88.39$ J/mol, $\tau = 395.5$ s, and $\beta = 0.75$. Table 1 lists the values of $\Delta H_T^{\text{eq.}}$, τ and β for $T = 569$, 565, 561, and 557 K, respectively. The temperature dependence of the relaxation time τ is shown in an Arrhenius plot in Fig. 5. In this representation, the data can well be fitted by a straight line, indicating that the relaxation time τ for the enthalpy relaxation from the glass into the supercooled liquid state follows an Arrhenius behavior $\tau = \tau_0 \exp(E/k_B T)$ with k_B the Boltzmann constant and $E = 3.96$ eV the apparent activation energy. The relaxation time increases exponentially with decreasing the temperature, making the equilibrium inaccessible at even lower annealing temperatures. Apparently, an Arrhenius behavior cannot hold over a wide temperature range for the $Pd_{43}Ni_{10}Cu_{27}P_{20}$ alloy.

The glass transition is widely viewed as kinetic freezing of a supercooled liquid, which depends on the cooling rate [17]. On the other hand, the relaxation of a glass into the supercooled liquid during reheating also depends on the experimental time scales, i.e. R_h. Therefore, the heating rate dependence of the glass transition can also be used to investigate the relaxation

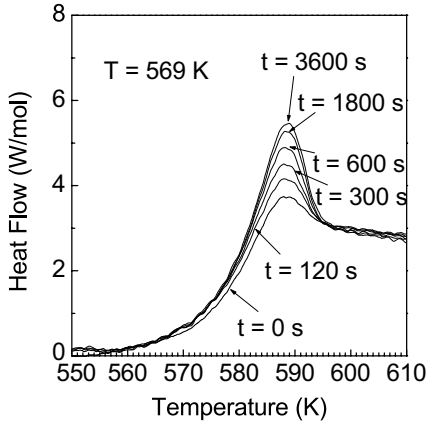

Fig. 3. DSC scans performed with $R_h = 0.167$ K/s after isothermal annealing at $T = 569$ K for different times, as indicated in the figure.

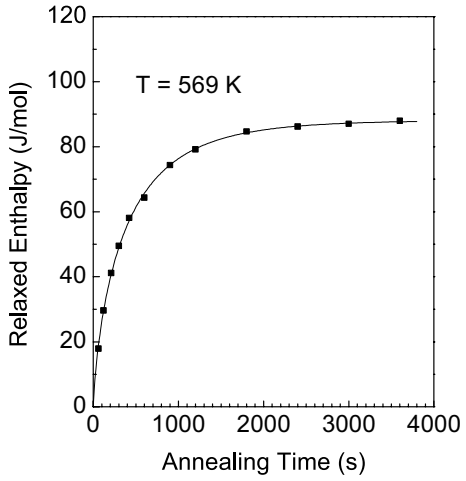

Fig. 4. Enthalpy relaxation as a function of annealing time t for $T = 569$ K. The solid line is a fit to the data, using Eq. (1).

Table 1
Fitting parameters $\Delta H_T^{\text{eq.}}$, τ, and β using Eq. (1) for $T = 569$, 565, 561, and 557 K, respectively

Annealing temperature T (K)	$\Delta H_T^{\text{eq.}}$ (J/mol)	τ (s)	β
569	88.39	395.5	0.75
565	136.46	698.3	0.69
561	188.42	1262.9	0.68
557	245.03	2237.4	0.7

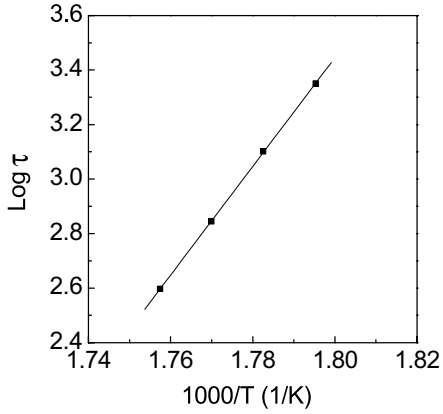

Fig. 5. Arrhenius plot of the relaxation time as a function of the inverse annealing temperature.

of a glass into the supercooled liquid [2,19,20]. Fig. 6 shows DSC scans of $Pd_{43}Ni_{10}Cu_{27}P_{20}$ performed with different heating rates ranging from 0.0167 to 5 K/s. With increasing heating rate, the onset of the glass transition temperature increases, which shows that the glass needs to reach a higher temperature to relax into the supercooled liquid state when the experimental time scale decreases. Fig. 7 shows the onset of the glass transition temperature T_g^{on} of the $Pd_{43}Ni_{10}Cu_{27}P_{20}$ alloy as a function of the heating rate R_h. The heating rate R_h as a function of T_g^{on} can be described by a Vogel–Fulcher like equation [21–23]

$$R_h = A \exp \frac{DT_g^0}{T_g^0 - T_g^{on}} \tag{2}$$

with A, D, and T_g^0 the fitting parameters. The temperature T_g^0 describes the onset of the glass transition in the limit of $R_h \to 0$. The best fit to the experimental data yields $A = 36.9$, $D = 0.303$, and $T_g^0 = 543.4$ K.

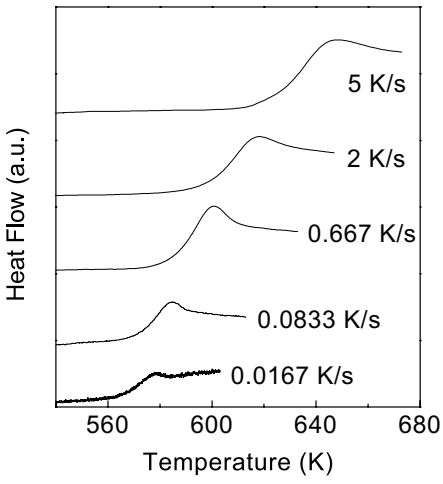

Fig. 6. DSC scans performed with different heating rates R_h, showing a shift of the glass transition temperature.

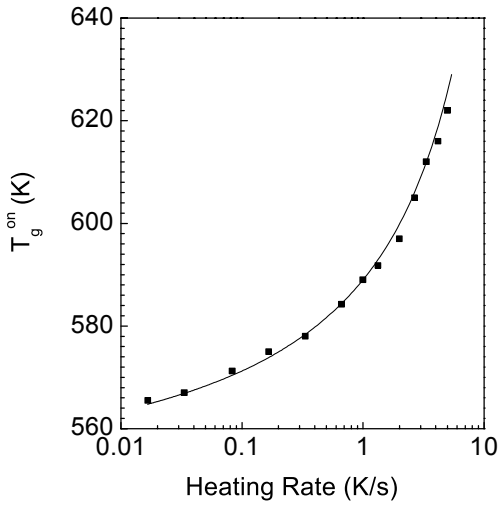

Fig. 7. Onset of the glass transition temperature, T_g^{on}, as a function of heating rate R_h. The solid line is a fit using Eq. (2).

4. Discussion

The enthalpy and entropy difference between the supercooled liquid state and the crystalline state as a function of temperature can be calculated from the specific heat capacity data of the supercooled liquid and the crystalline counterpart. The specific heat capacity of an equilibrium supercooled liquid above T_g can be measured directly by DSC when the experimental time scales are longer than the internal relaxation times of the liquid. In the range of the calorimetric glass transition, the equilibrium value cannot be measured using DSC, since the supercooled liquid cannot reach equilibrium at the time scale of conventional DSC experiments. However, enthalpy relaxation (or enthalpy recovery) experiments can be performed at long time scales. In this case, the specific heat capacity data of the amorphous state can relax into the equilibrium supercooled liquid state after extended isothermal annealing. Considering that the enthalpy difference (relaxed at different temperatures T_1 and T_2) is due to the specific heat capacity difference between the supercooled liquid state and the amorphous state [24], the specific heat capacity c_p at the temperature $(T_1 + T_2)/2$ is

$$c_p = c_p^{am.} + \frac{\Delta H_{T_1}^{eq.} - \Delta H_{T_2}^{eq.}}{T_1 - T_2}, \tag{3}$$

where $c_p^{am.}$ is the specific heat capacity of the glass at the temperature $(T_1 + T_2)/2$, and $\Delta H_{T_1}^{eq.}$ and $\Delta H_{T_2}^{eq.}$ are the enthalpies at T_1 and T_2 for infinitely long relaxation times. The calculated specific heat capacity data from the enthalpy relaxation measurements are plotted in Fig. 8 together with the data determined by DSC. The specific heat capacity data of the undercooled liquid were fitted using [12,25]

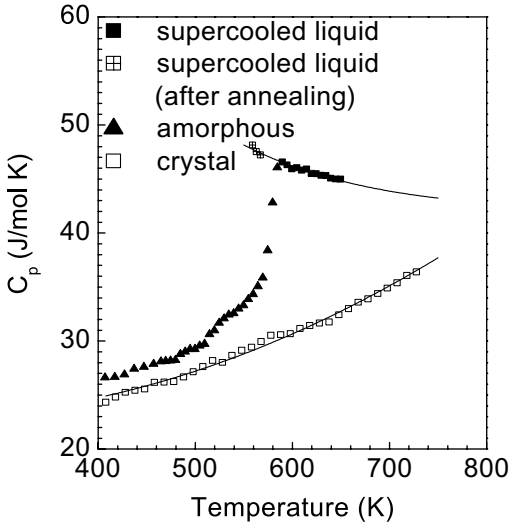

Fig. 8. Specific heat capacity in the supercooled liquid, amorphous, and crystalline state as a function of temperature. The data range for the specific heat capacity in the supercooled liquid state was extended by the results of the enthalpy relaxation experiments. The solid lines are fits using Eqs. (4) and (5).

$$c_{\mathrm{p}}^{\mathrm{l}}(T) = 3R + aT + bT^{-2}, \tag{4}$$

with $R = 8.314$ J mol^{-1} K^{-1}. The specific heat capacity data of the crystal were fit using the equation

$$c_{\mathrm{p}}^{\mathrm{x}}(T) = 3R + cT + dT^{2}. \tag{5}$$

The resulting fitting parameters are $a = 0.0128$ J mol^{-1} K^{-2}, $b = 4.89 \times 10^{6}$ J mol^{-1} K, $c = -0.0204$ J mol^{-1} K^{-2}, and $d = 5 \times 10^{-5}$ J mol^{-1} K^{-3}, respectively.

The enthalpy and the entropy changes of the equilibrium supercooled liquid with respect to the crystal were then calculated from the fitted specific heat capacity data, using

$$\Delta H^{\mathrm{l\text{-}x}}(T) = \Delta H_{\mathrm{f}} - \int_{T}^{T_{\mathrm{m}}} \left[c_{\mathrm{p}}^{\mathrm{l}}(T) - c_{\mathrm{p}}^{\mathrm{x}}(T)\right] \mathrm{d}T, \tag{6}$$

$$\Delta S^{\mathrm{l\text{-}x}}(T) = \Delta S_{\mathrm{f}} - \int_{T}^{T_{\mathrm{m}}} \frac{c_{\mathrm{p}}^{\mathrm{l}}(T) - c_{\mathrm{p}}^{\mathrm{x}}(T)}{T} \mathrm{d}T, \tag{7}$$

with ΔH_{f} and ΔS_{f} the enthalpy and entropy of fusion, respectively. Fig. 9 shows the calculated $\Delta H^{\mathrm{l\text{-}x}}(T)$ and $\Delta S^{\mathrm{l\text{-}x}}(T)$ scaled with the respective values at the melting temperature T_{m}. The enthalpy and the entropy differences of the supercooled liquid with respect to the crystal decrease with temperature. However, the enthalpy and the entropy of a supercooled liquid cannot be smaller than that of the corresponding crystal [26]. This thermodynamic crisis is averted by the experimentally observed glass transition. The isenthalpic temperature and the isentropic temperature (or widely known as Kauzmann temperature T_{K}) were determined to be 384 and 447 K, respectively. Fig. 9 shows that the enthalpy of the $Pd_{43}Ni_{10}Cu_{27}P_{20}$ supercooled liquid decreases less

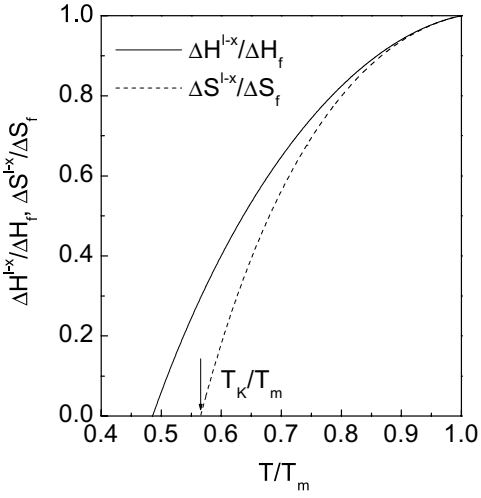

Fig. 9. Temperature dependence (T/T_{m}) of excess enthalpy (solid line) and excess entropy (dashed line) normalized with the respective values at the melting temperature.

rapidly with decreasing temperature than the entropy, implying that the entropic crisis is more prominent than the enthalpic one. Therefore, the Kauzmann temperature T_{K} sets the ultimate thermodynamic bound for the glass transition. Since a fragile liquid has a larger difference in the specific heat capacity between the supercooled liquid and the crystal [16], the entropy of a fragile liquid is expected to decrease more rapidly with decreasing temperature than the entropy of a strong liquid. Thus, a correlation between thermodynamic fragility and kinetic fragility is expected and has indeed been found in molecular and ionic glass-forming liquids [27,28], and recently in metallic glass-forming liquids [29].

According to classical nucleation theory, the steady-state crystal nucleation rate per unit volume, I_{ss}, is determined by both kinetics and thermodynamics, which can be expressed by [30]

$$I_{\mathrm{ss}} = \frac{A}{\eta(T)} \exp\left[-\frac{16\pi\sigma^{3}}{3k_{\mathrm{B}}T[\Delta G^{\mathrm{l\text{-}x}}(T)]^{2}}\right] \tag{8}$$

with A a constant, $\eta(T)$ the temperature dependence of the viscosity of the supercooled liquid, σ the interfacial energy between the liquid and the crystal, and $\Delta G^{\mathrm{l\text{-}x}}(T)$ the Gibbs free energy difference between the liquid and the crystal. The interplay between kinetics and thermodynamics results in a maximum of I_{ss} at some intermediate undercooling. Bulk metallic glass-forming liquids are expected to have a higher viscosity around the melting point and a lower driving force $\Delta G^{\mathrm{l\text{-}x}}(T)$ for crystal nucleation. Indeed, bulk metallic glasses like Vit 1 and Vit 4 have a viscosity of around 10 Pa s at the melting point, which is 10^{3} times higher than that of ordinary metallic liquids [3,31,32]. The viscosity of metallic liquids around the melting point is generally

correlated with the liquid fragility, which measures the degree with which the viscosity of a supercooled liquid deviates from the Arrhenius behavior. A strong liquid usually has a higher viscosity at the melting point than a fragile one. There are different ways to quantify the liquid fragility [33,34]. Recently, we derived a fitting equation for viscosity with a simple form $\eta = \eta_0 \exp(E/k_B T) \exp(\Phi T/T_g)$, where E is the activation energy for viscous flow at low temperatures, and Φ represents the fragility of a glass-forming system [34]. Another measure of the liquid fragility index m has been quantified as [33]

$$m = \left.\frac{\mathrm{d}\log\eta}{\mathrm{d}\left(T_{g,\eta}/T\right)}\right|_{T=T_{g,\eta}}, \tag{9}$$

where $T_{g,\eta}$ is the temperature at which the viscosity η of a supercooled liquids reaches 10^{12} Pa s. It was pointed out that there is a good correlation between Φ and m [34]. Bulk metallic glasses like Vit 1 and Vit 4 show strong liquid behavior [3,31]. Such strong liquids typically have a fragility index m of less than 50. The calculation of the fragility index m based on Eq. (9) needs the determination of the fitting parameters D and T_g^0 in Eq. (2). As shown in Fig. 7, the fitting parameters D and T_g^0 can be obtained from the heating rate dependence of the glass transition temperature. The fragility index m is then given by

$$m = \frac{DT_g^0 T_{g,\eta}}{\left(T_{g,\eta} - T_g^0\right)^2 \ln 10}. \tag{10}$$

Viscosity measurements [35] show that $T_{g,\eta}$ is equal to 568.3 K for $Pd_{43}Ni_{10}Cu_{27}P_{20}$, which results in a fragility index m of 65. This shows that $Pd_{43}Ni_{10}Cu_{27}P_{20}$ is a relatively fragile liquid! This is quite surprising since the $Pd_{43}Ni_{10}Cu_{27}P_{20}$ alloy shows the best glass-forming ability found so far. The good glass-forming ability of Zr- and Mg-based alloys, for example, is generally attributed to a strong liquid behavior and a low thermodynamic driving force for crystal nucleation [2,3,12,13].

To determine the correlation between fragility and glass-forming ability, the fragility index m was calculated in the present study from viscosity data of several metallic glass-forming liquids [3,31,36–39]. Generally, a good correlation between critical cooling rate, which determines the glass-forming ability, and fragility index m has been found, as is shown in Fig. 10. The Pd-based alloys, however, show significantly lower critical cooling rates than expected from their measured fragility index [13,35,40]. Thus, the viscosity does not appear to be responsible for the good glass-forming ability of Pd-based alloys, in contrast to all other bulk metallic glass formers.

A further parameter influencing glass-forming ability is the driving force for crystal nucleation (see Eq. (8)), which was calculated for $Pd_{43}Ni_{10}Cu_{27}P_{20}$ from the

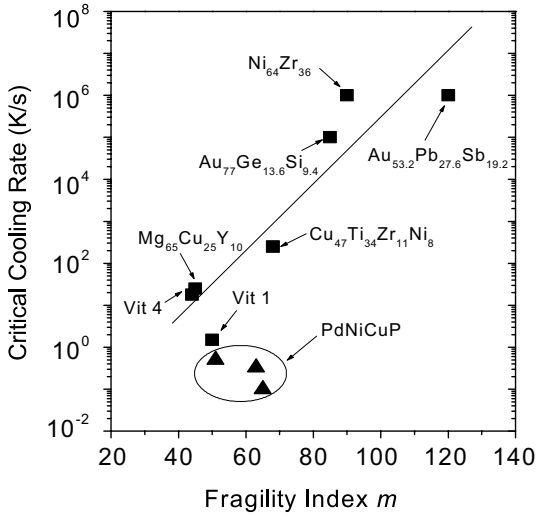

Fig. 10. Relationship between critical cooling rate for glass formation and kinetic fragility index m for different metallic glass-forming alloys. The solid line serves as a guide for the eye.

temperature dependencies of the enthalpy and entropy changes (Eqs. (6) and (7)). The Gibbs free energy difference between liquid and crystal, $\Delta G^{l-x}(T)$, as a function of temperature is plotted in Fig. 11 together with values of other bulk metallic glass-forming liquids [2,12,36,38,41–43]. It is evident that the $Pd_{43}Ni_{10}Cu_{27}P_{20}$ alloy has a very low driving force for crystal nucleation, which is even lower than that of $Zr_{41.2}Ti_{13.8}Cu_{12.5}Ni_{10}Be_{22.5}$ (Vit1), which has a critical cooling rate of 1 K/s. Thus, it appears that $\Delta G^{l-x}(T)$ is the decisive factor for the excellent glass-forming ability of $Pd_{43}Ni_{10}Cu_{27}P_{20}$. In addition, most of the alloys following the straight line in Fig. 10 crystallize as nanocrystals in an

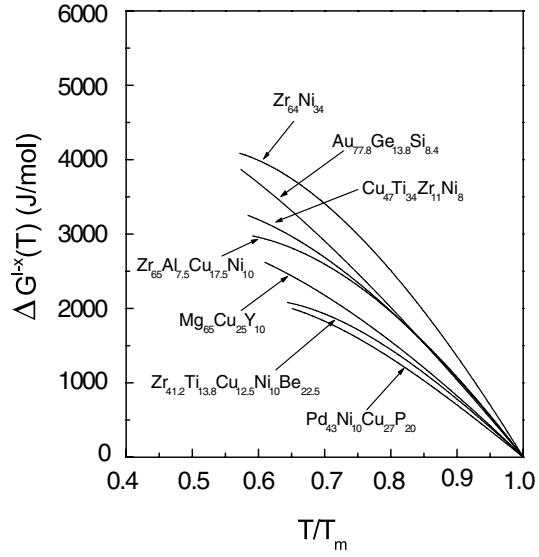

Fig. 11. Comparison of the Gibbs free energy difference between liquid and crystal as a function of temperature for different metallic glass-forming alloys.

amorphous matrix in the deeply undercooled liquid range [44]. In contrast, the primary crystals in the Pd-based alloys are much larger and no phase separation is detected on the nanometer scale [44]. Thus, it appears that the diffusion lengths necessary for primary crystallization are larger in the Pd-based alloys than in all other bulk metallic glass-forming systems, which may be an additional factor contributing to the excellent glass-forming ability of Pd-based alloys.

Furthermore, there appears to be a correlation between the Kohlrausch exponent β and the fragility index m in glass-forming liquids. Early studies of enthalpy relaxation and recovery focused on organic and inorganic glassy materials [4]. In metallic glass systems, enthalpy relaxation phenomena were investigated by Chen [45] in $Pd_{48}Ni_{32}P_{20}$, Sommer et al. [46] in $Cu_{67}Ti_{33}$ and other binary systems, and Koebrugge et al. [47] in $Pd_{40}Ni_{40}P_{20}$. The enthalpy relaxation and recovery near T_g was also studied recently in bulk metallic glass-forming liquids [24]. The relaxation from the amorphous state into the equilibrium supercooled liquid state usually shows a stretched exponential behavior (Fig. 4), with the resulting Kohlrausch exponent β being closely related to the distribution of the Debye relaxation times (a lower value of β indicates a wider distribution) [18]. On the other hand, the fragility indicates the degree of structural inhomogeneity in a supercooled liquid. Therefore, one may expect a correlation between the Kohlrausch exponent β and the fragility index m, with fragile liquids having a lower value of β. Indeed, the more fragile liquid $Pd_{43}Ni_{10}Cu_{27}P_{20}$ ($m = 65$, $\beta = 0.7$) has a lower Kohlrausch exponent than Vit 1 ($m = 50$, $\beta = 0.8$ [3]). Such a correlation has also been found in some covalent, ionic, and polymeric glasses near the glass transition [33].

5. Summary

The thermodynamics, enthalpy relaxation, and the fragility of a $Pd_{43}Ni_{10}Cu_{27}P_{20}$ bulk metallic glass-forming liquid have been investigated. In contrast to other bulk metallic glass-forming liquids, $Pd_{43}Ni_{10}Cu_{27}P_{20}$ was found to exhibit a relatively fragile liquid behavior, although this alloy has so far the lowest critical cooling rate for glass formation. The glass-forming ability of this alloy is discussed within the context of classical nucleation theory. The good glass-forming ability of this alloy is attributed to a lower driving force for nucleation and larger diffusion lengths for crystallization in comparison to other bulk glass-forming systems. The enthalpy relaxation from the amorphous state into the equilibrium supercooled liquid state of this alloy displays a stretched exponential behavior at temperatures around the glass transition with a Kohlrausch exponent $\beta = 0.7$. The relaxation time of the $Pd_{43}Ni_{10}Cu_{27}P_{20}$ alloy from the glass into the supercooled liquid state was found to obey an Arrhenius law with an apparent activation energy of 3.96 eV.

Acknowledgements

This work was supported by start-up funds from University of California, Davis (J.F. Löffler), the Deutsche Forschungsgemeinschaft (G.W. Leibniz Program), the German Space Agency (DLR Grant No. 50 WM 0041), the European Space Agency (ESA MAP AO-99-022) and the European Bulk Metallic Glass project (BMG HPRN-CT-2000-00033).

References

[1] Angell CA. Science 1995;267:1924.
[2] Fecht H-J. Mater Trans JIM 1995;36:777.
[3] Busch R, Bakke E, Johnson WL. Acta Mater 1998;46:4725.
[4] Hodge IM. J Non-Cryst Solids 1994;169:211.
[5] Inoue A, Zhang T, Masumoto T. Mater Trans JIM 1990;31:425.
[6] Inoue A, Kato A, Zhang T, Kim SG, Masumoto T. Mater Trans JIM 1991;32:609.
[7] Zhang T, Inoue A, Masumoto T. Mater Trans JIM 1991;32:1005.
[8] Peker A, Johnson WL. Appl Phys Lett 1993;63:2342.
[9] Nishiyama N, Inoue A. Mater Trans JIM 1996;37:1531.
[10] Inoue A, Makino A, Mizushima. J Magn Man Mater 2000;215–216:246.
[11] Fan GJ, Löser W, Roth S, Eckert J, Schultz L. J Mater Res 2000;15:1556.
[12] Busch R, Kim YJ, Johnson WL. J Appl Phys 1995;77:4039.
[13] Wilde G, Görler GP, Willnecker R, Fecht H-J. J Appl Phys 2000;87:1141.
[14] Lu I-R, Wilde G, Görler GP, Willnecker R. J Non-Cryst Solids 1999;250–252:577.
[15] Fecht HJ, Perepezko JH, Lee MC, Johnson WL. J Appl Phys 1990;68:4494.
[16] Angell CA. J Phys Chem Solids 1988;49:863.
[17] Jäckle J. Physica B & C 1984;127:79.
[18] Palmer RG, Stein DL, Abrahams E, Anderson PW. Phys Rev Lett 1984;53:958.
[19] Moynihan CT, Easteal AJ, Wilder J, Tucker J. J Phys Chem 1974;78:2673.
[20] Bürning R, Samwer K. Phys Rev B 1992;46:11318.
[21] Vogel W. Phys Z 1921;22:645.
[22] Tammann G, Hesse G. Z Anorg Allg Chem 1926;156:245.
[23] Fulcher GS. J Am Ceram Soc 1925;8:339.
[24] Busch R, Johnson WL. Appl Phys Lett 1998;72:2695.
[25] Kubaschewski O, Alcock CB, Spencer PJ. Materials Thermochemistry. 6th ed. New York: Permagon; 1993.
[26] Kauzmann AW. Chem Rev 1948;43:219.
[27] Ito K, Moynihan CT, Angell CA. Nature 1999;398:492.
[28] Martinez L-M, Angell CA. Nature 2001;410:663.
[29] Fan GJ, Wunderlich RK, Fecht H-J. Mat Res Soc Symp Proc 2003;754:CC5.9.1.
[30] Herlach DM. Mater Sci Eng 1994;R12:177.
[31] Waniuk TA, Busch R, Masuhr A, Johnson WL. Acta Mater 1998;46:5229.
[32] Johnson WL. MRS Bull 1999;24:42.
[33] Böhmer R, Ngai KL, Angell CA, Plazek DJ. J Chem Phys 1993;99:4201.

[34] Fan GJ, Fecht H-J. J Chem Phys 2002;116:5002.
[35] Fan GJ, Fecht H-J., to be published.
[36] Chen HS, Turnbull D. J Chem Phys 1968;48:2560.
[37] Klose G, Fecht H-J. Mater Sci Eng 1994;A179/A180:77.
[38] Busch R, Liu W, Johnson WL. J Appl Phys 1998;83:4134.
[39] Glade SC, Johnson WL. J Appl Phys 2000;87:7249.
[40] Nishiyama N, Inoue A. Mater Trans JIM 1999;40:64.
[41] Glade SC, Busch R, Lee DS, Johnson WL, Wunderlich RK, Fecht H-J. J Appl Phys 2000;87:7242.
[42] Wunderlich RK, Lee DS, Johnson WL, Fecht H-J. Phys Rev B 1997;55:26.
[43] Wunderlich RK, Fecht H-J. Mater Trans JIM 2001;42:565.
[44] Löffler JF, Johnson WL, Wagner W, Thiyagarajan P. Mater Sci Forum 2000;343–346:179.
[45] Chen HS. J Non-Cryst Solids 1981;46:289.
[46] Sommer F, Haas H, Predel B. J Non-Cryst Solids 1984;61&62:793.
[47] Koebrugge GW, Sietsma J, van den Beukel A. Acta Metall Mater 1992;40:753.